

Supporting Information

A nano-truncated Ni/La doped manganese spinel material for high rate performance and long cycle life lithium-ion batteries

Meng Li,^{ab1} Yan Li,^{ab1} Yujiao Guo,^{ab} Junming Guo,*^{ab} Mingwu Xiang, *^{ab} Wei Bai,^{ab} Xiaofang Liu^{ab} and Hongli Bai^{ab}

^a National and Local Joint Engineering Research Center for Green Preparation Technology of Biobased Materials, Yunnan Minzu University, Kunming, 650500, China

^b Key Laboratory of Green-chemistry Materials in University of Yunnan Province, Yunnan Minzu University, Kunming, 650500, China

¹ Meng Li and Yan Li are co-first authors of the article.

corresponding author E-mail addresses: guojunming@tsinghua.org.cn (J. M. Guo), xmwbboy@163.com (M. W. Xiang).

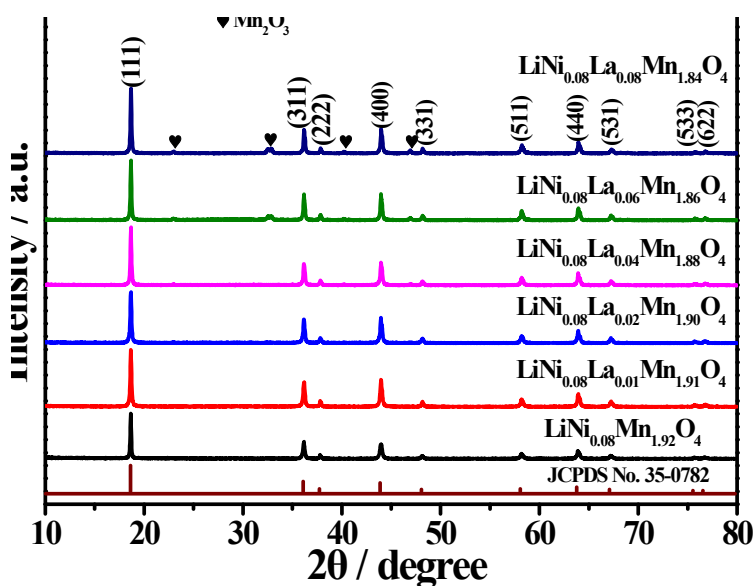


Fig. S1. XRD patterns of the $\text{LiNi}_{0.08}\text{La}_x\text{Mn}_{1.92-x}\text{O}_4$ ($x=0, 0.01, 0.02, 0.04, 0.06, 0.08$) samples.

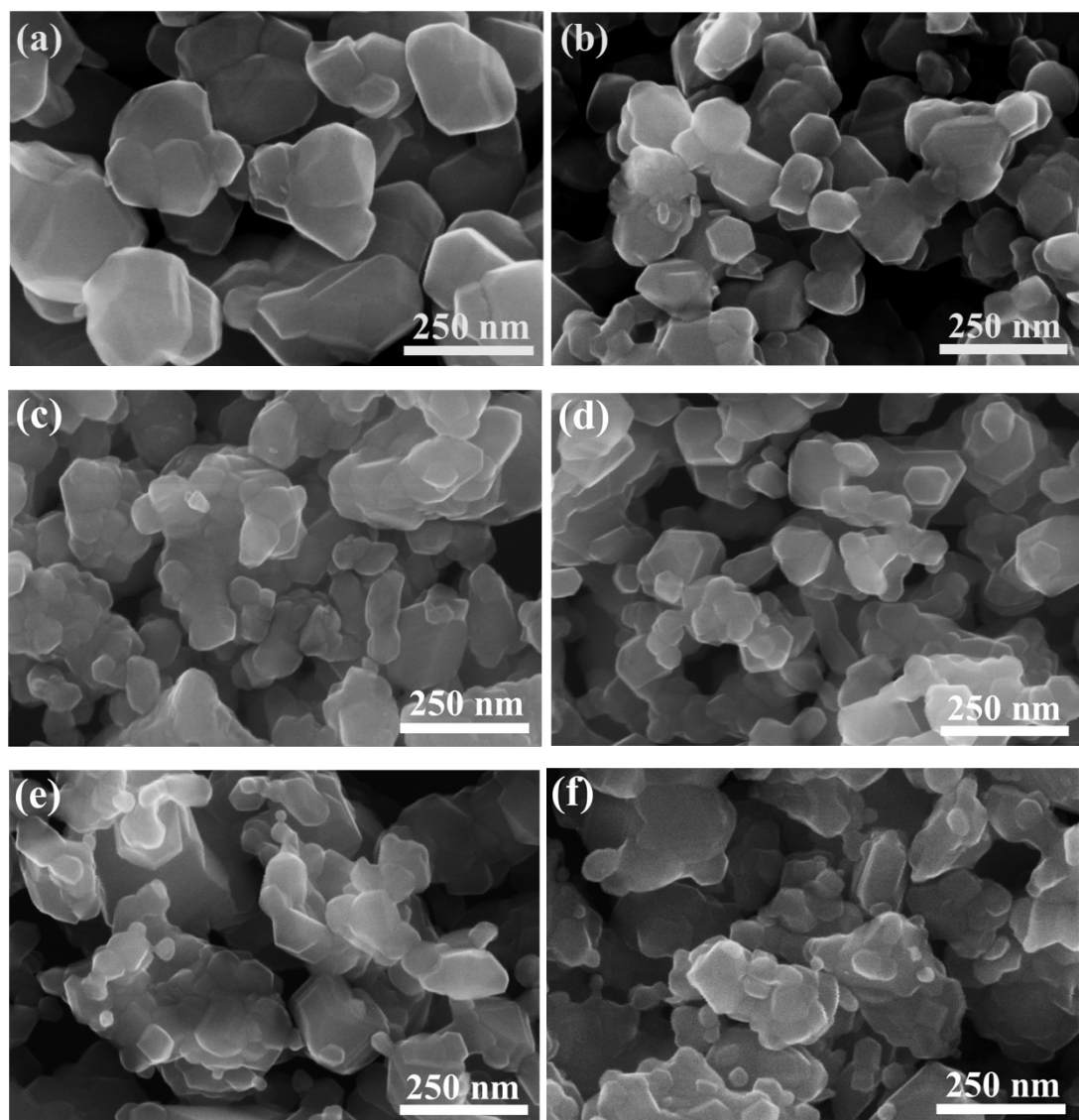


Fig. S2. SEM images of the $\text{LiNi}_{0.08}\text{La}_x\text{Mn}_{1.92-x}\text{O}_4$ samples: (a) $x=0$, (b) $x=0.01$, (c) $x=0.02$, (d) $x=0.04$, (e) $x=0.06$ and (f) $x=0.08$.

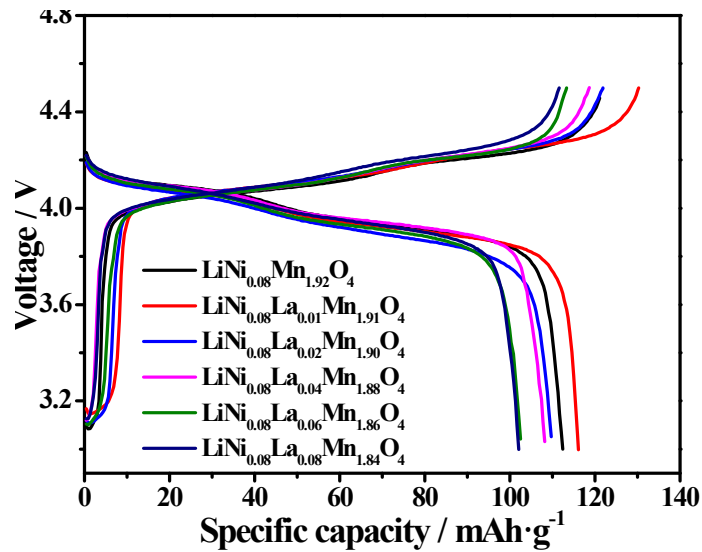


Fig. S3. first charge/discharge curves of the $\text{LiNi}_{0.08}\text{La}_x\text{Mn}_{1.92-x}\text{O}_4$ ($x=0, 0.01, 0.02, 0.04, 0.06, 0.08$) samples at 1 C.

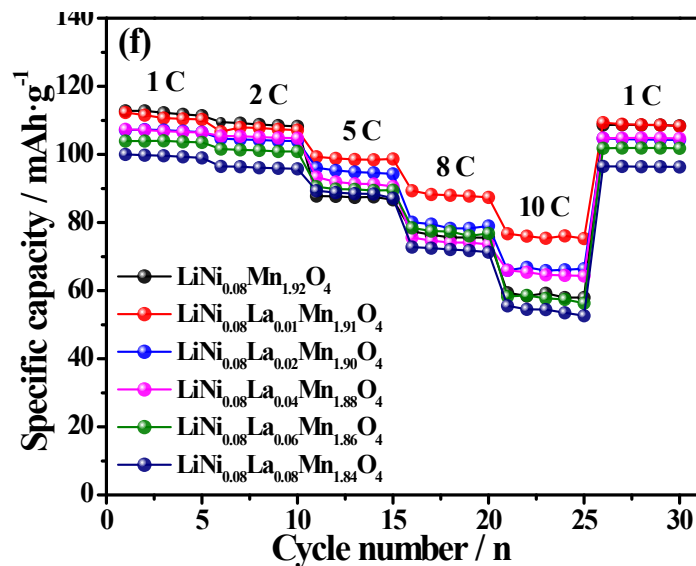


Fig. S4. rate performances of the $\text{LiNi}_{0.08}\text{La}_x\text{Mn}_{1.92-x}\text{O}_4$ ($x=0, 0.01, 0.02, 0.04, 0.06, 0.08$) samples.

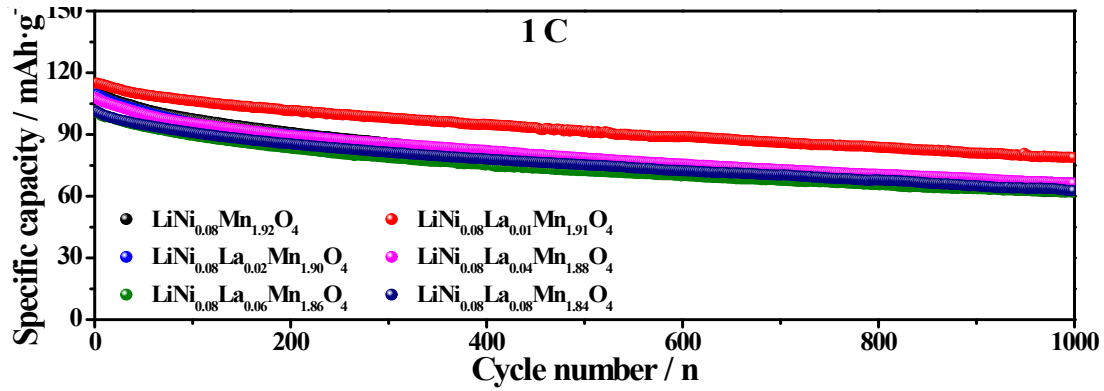


Fig. S5. cycling performances of the $\text{LiNi}_{0.08}\text{La}_x\text{Mn}_{1.92-x}\text{O}_4$ ($x=0, 0.01, 0.02, 0.04, 0.06, 0.08$) samples at 1 C.

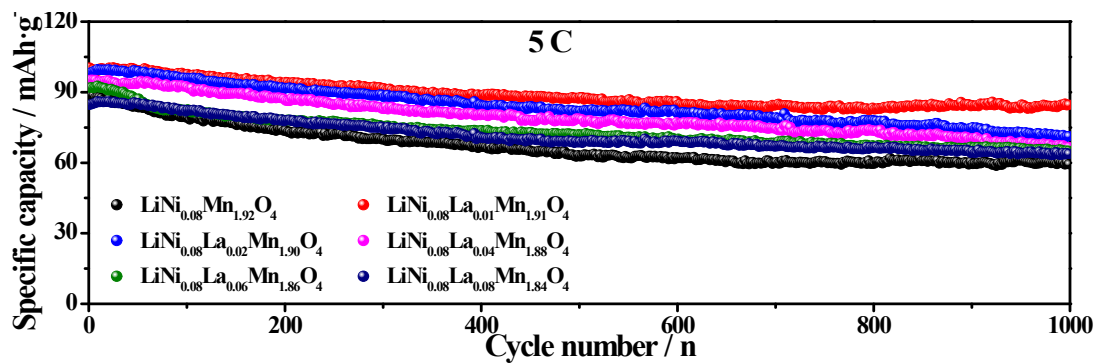


Fig. S6. cycling performances of the $\text{LiNi}_{0.08}\text{La}_x\text{Mn}_{1.92-x}\text{O}_4$ ($x=0, 0.01, 0.02, 0.04, 0.06, 0.08$) samples at 5 C.

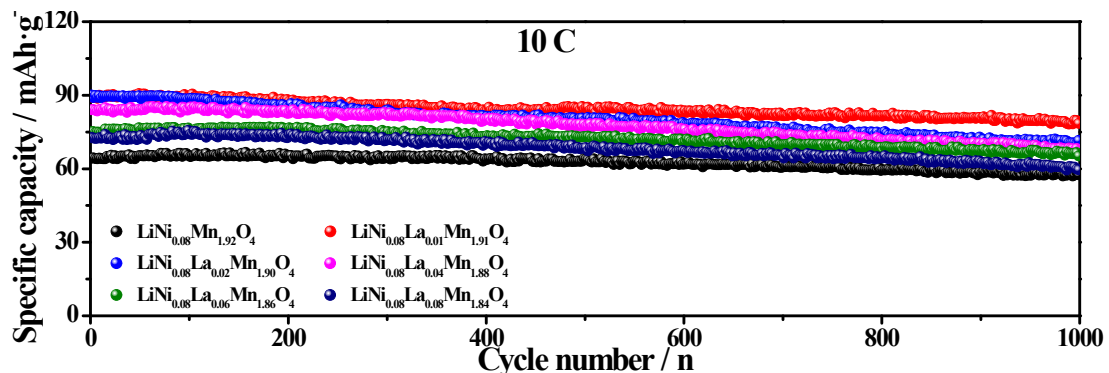


Fig. S7. cycling performances of the $\text{LiNi}_{0.08}\text{La}_x\text{Mn}_{1.92-x}\text{O}_4$ ($x=0, 0.01, 0.02, 0.04, 0.06, 0.08$) samples at 10 C.

The calculation of the lithium ion diffusion coefficient (D_{Li^+}):

The corresponding Randles-Sevcik formula is as follows:¹

$$i_p = (2.69 \times 10^5) n^{3/2} C_{\text{Li}^+} A D_{\text{Li}^+}^{1/2} V^{1/2} \quad (25^\circ\text{C}) \quad (1)$$

in the equation, i_p stands the peak current value (A), the electron transfer number n is 1, C_{Li^+} denotes the Li^+ volume concentration ($0.024 \text{ mol} \cdot \text{cm}^{-3}$), A means the electrode superficial area (2.01

cm^2), and v is the scan speed ($\text{V}\cdot\text{s}^{-1}$). The D_{Li^+} value is computed though the fitting linear connection between i_p and $v^{1/2}$ (Fig. S8).

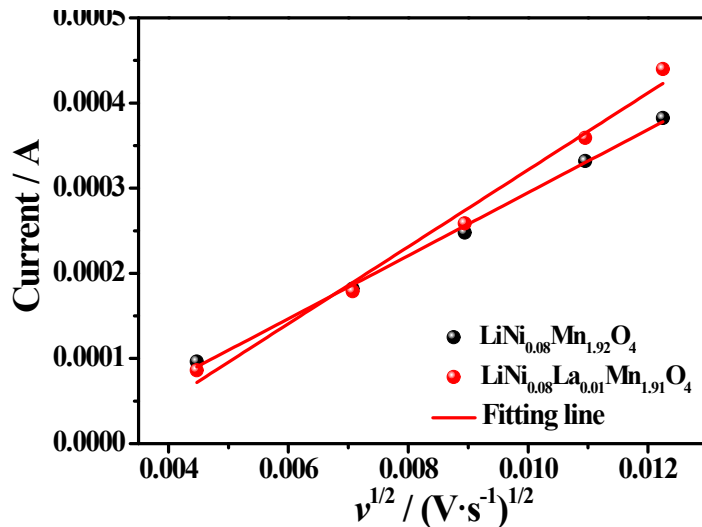


Fig. S8. Fitting plots about peak current vs. square root of scan rate for $\text{LiNi}_{0.08}\text{Mn}_{1.92}\text{O}_4$ and $\text{LiNi}_{0.08}\text{La}_{0.01}\text{Mn}_{1.91}\text{O}_4$ samples.

The calculation of the apparent activation energy (E_a):

The E_a value is calculated on the basis of EIS data at different temperatures from the following formulas:²

$$i_0 = RT/nFR_{ct} \quad (2)$$

$$i_0 = A \exp(-E_a/RT) \quad (3)$$

where, i_0 expresses exchange current (A), the gas constant value of R is $8.314 \text{ J}\cdot\text{mol}^{-1}\cdot\text{K}^{-1}$, T means absolute temperature (K), the electron transfer number n is 1, the Faraday constant value of F is $96484.5 \text{ C}\cdot\text{mol}^{-1}$, and A is an independent coefficient of temperature. According to the aforementioned (2) and (3) formulas, the E_a can be stated as $E_a = -Rk\ln 10$ (k denotes the slope of the fitting line in Fig. S9). The E_a value can be further calculated.

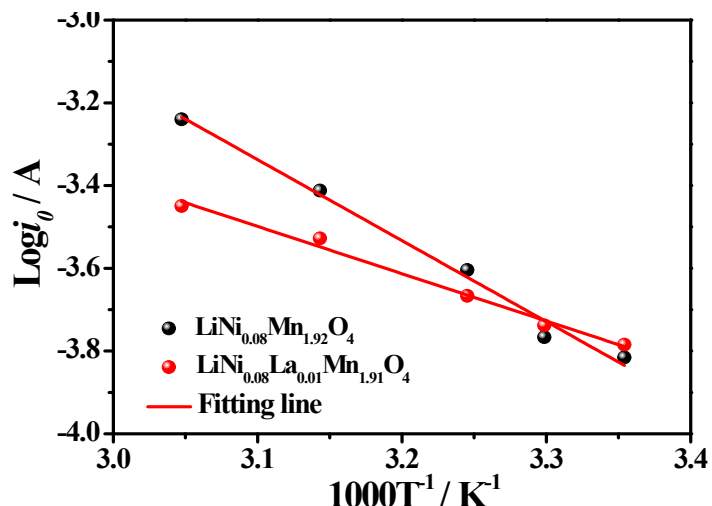


Fig. S9. Arrhenius plots about $\log i_0$ vs. $1000T^{-1}$ for $\text{LiNi}_{0.08}\text{Mn}_{1.92}\text{O}_4$ and $\text{LiNi}_{0.08}\text{La}_{0.01}\text{Mn}_{1.91}\text{O}_4$ samples.

References

- 1 Y. J. Cai, Y. D. Huang, X. C. Wang, D. Z. Jia, W. K. Pang, Z. P. Guo, Y. P. Du, X and C. Tang, *J. Power Sources*, 2015, 278, 574–581.
- 2 S. L. Chou, J. Z. Wang, H. K. Liu, S. X. Dou, *J. Phys. Chem. C*, 2011, 115, 16220–16227.